# Pepsinogen Activation: Genesis of the Binding Site†

David M. Glick,*,‡ Henry E. Auer,*,‡,§ Daniel H. Rich,‖ Megumi Kawai,‖ and Ashwini Kamath‡

*Department of Biochemistry, The Medical College of Wisconsin, Milwaukee, Wisconsin 53226, and School of Pharmacy, The University of Wisconsin, Madison, Wisconsin 53706*

*Received September 10, 1985; Revised Manuscript Received October 29, 1985*

ABSTRACT: Previous experiments have suggested that a substrate binding site may appear relatively early in the sequence of transformations that pepsinogen undergoes during its unimolecular activation. To test this possibility, *tert*-Boc-L-valyl-[3(*S*)-hydroxy-4(*S*)-amino-5-(2-naphthyl)pentanoyl]-L-alanylisoamylamide, a fluorescent analogue of pepstatin, has been used to measure the rate of appearance of the binding site. This probe is a potent inhibitor of pepsin, and its naphthyl group is an environmentally sensitive fluorophore that permits binding to be detected by fluorescence spectroscopy. In stopped-flow experiments, the fluorescence change following acidification of pepsinogen due to binding of the probe was found to obey a two-term exponential decay law. Analysis of the data obtained at various pH values permits us to rule out a sequential model for the kinetics. Rather, we were able to demonstrate that a concurrent model, with two species undergoing simultaneous transformation at different rates, is consistent with the results. The two species are related to each other by the protonation of a single site with a $pK_a$ of approximately 2.2. We obtained essentially identical results in an analysis of the early events observed in the acidification of pepsinogen labeled with 6-(*p*-toluidinyl)naphthalene-2-sulfonyl chloride (Auer & Glick, 1984). The protonic equilibrium probably occurs early after exposure to acid and is proposed to lead to a conformational change that freezes the distribution between the two species. It may be that these two conformers persist as identifiable entities at later stages of activation as well. In accord with this hypothesis, we find the Arrhenius energy of activation for the conversion to alkaline lability to vary over a range of pH values.

We have been seeking to characterize in quantitative terms the complete sequence of events involved in the activation of pepsinogen to pepsin upon exposure to acid. Within 5–100 ms of acidification, pepsinogen undergoes changes in fluorescence that were interpreted as arising from conformational changes (Auer & Glick, 1984). Two concurrent processes were characterized in TNS-pepsinogen,[1] which appear to occur in protein species differing from each other by a single protonation. These rapid processes were insensitive to the presence of pepstatin. No further changes in fluorescence were observed prior to time scales of 2–5 s. The next well-characterized step in the activation process is the conversion to alkaline lability. This is generally understood to represent cleavage of the activation peptide from the amino terminus of the pepsinogen molecule. The half-time for this process is in the range of 30 s (Al-Janabi et al., 1972). Nevertheless, the peptides produced in this step remain complexed to the nascent enzyme for some time longer, being released at about one-fifth or less that rate (Twining et al., 1981; Glick et al., 1982). It is only at this stage that the free enzyme molecule is produced.

One aspect of the activation process that has not yet been studied is the rate of emergence of the binding site for the amino acid sequence around the scissile bond. Certain findings reported in the literature suggested to us that this might be accessible to investigation. First, Tang and co-workers showed that upon acidification, pepsinogen adsorbs to pepstatin immobilized on Sepharose (Marciniszyn et al., 1976). If the resin was then developed at pH 8, some unchanged and some denatured zymogen was recovered. They concluded that the ability to bind pepstatin arises quite early in the sequence of activation events. Second, we observed that inclusion of pepstatin with the zymogen during activation retards the dissociation of the activation peptide. This led us to the same conclusion, namely, that pepstatin is binding to pepsinogen prior to cleavage of the peptide bond (Glick et al., 1982). This may seem paradoxical, since one would expect that the activation sequence should compete effectively with any inhibitor by virtue of its proximity to the binding site; it should bind and be cleaved as soon as the binding site is generated. In contrast to the observations with pepstatin and in accord with the latter presumption, Fruton measured the rate at which Mansyl-Phe-Phe-OPp (a poor substrate with high $K_m$) is bound during pepsinogen activation, by observing the enhancement of the fluorescence of the Mansyl group. He observed a half-time ($\tau_{1/2}$ = 25 s) that corresponds closely to the rate we measured for the dissociation of the activation peptide (Fruton, 1976; Twining et al., 1981). It is apparent that binding of Mansyl-Phe-Phe-OPp does not occur until the activation peptide departs from the binding site.

We noted above that a strong inhibitor, such as pepstatin, appears to bind to intermediates of pepsinogen before complete activation occurs. The application of analogues of ligands, substrates, and inhibitors in protein chemistry, enzymology, and biochemical pharmacology has led to enhanced understanding of protein structure and enzyme mechanisms. We therefore set out to determine whether Boc-L-Val-[3(*S*)-hydroxy-4(*S*)-amino-5-(2-naphthyl)pentanoyl]-L-Ala-Iaa

† This work was supported in part by USPHS Research Grant AM 20100 to D.H.R. and a grant from the Frasch Foundation to D.M.G.

‡ The Medical College of Wisconsin.

§ Present address: International Minerals & Chemical Corp., 1810 Frontage Rd., Northbrook, IL 60062.

‖ The University of Wisconsin.

[1] Abbreviations: Hanp, 3(*S*)-hydroxy-4(*S*)-amino-5-(2-naphthyl)-pentanoyl; Boc, *tert*-butyloxycarbonyl; Iaa, isoamylamide; Iva, isovaleryl; Mansyl, 6-(*N*-methylanilino)naphthalene-2-sulfonyl; P, pepsin; Pg, pepsinogen; Pp, 3-(4-pyridinium)propyl; TNS, 6-(*p*-toluidinyl)naphthalene-2-sulfonyl; $(NO_2)$Phe, *p*-nitrophenylalanyl.

0006-2960/86/0425-1858$01.50/0 

(compound I), a pepstatin analogue with the fluorescent

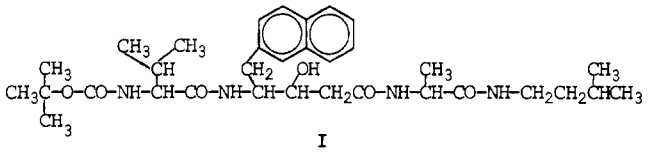

I

naphthyl group positioned to bind in the active site, can combine with pepsinogen prior to completion of the activation process. If so, we reasoned that the probe would adsorb to the protein as fast as the binding site became available and by its enhanced fluorescence would permit us to monitor the creation of the binding site. These experiments have indeed been successful, for they have permitted us to identify a new step in activation, the appearance of the binding site.

## Materials and Methods

Pig pepsinogen was purchased from Sigma Chemical Co. Its concentration was calculated from $\epsilon_{280} = 5.13 \times 10^4$ $M^{-1}$ $cm^{-1}$ (Arnon & Perlmann, 1963). Compound I was weighed on a Mettler microbalance and dissolved in methanol to serve as a stock solution to be added to solutions of pepsinogen or acid.

*Synthesis of Compound I.* Boc-Hanp-OEt was synthesized from Boc-$\beta$-naphthylalanine ethyl ester following a modification of the procedure developed for the synthesis of statine (Rich et al., 1978; Rich & Salituro, 1983): mp 164–165 °C as the cyclohexylammonium salt of the corresponding acid (Anal. Calcd for $C_{26}H_{38}O_5N_2$: C, 68.10; H, 8.35, N, 6.11. Found: C, 67.80; H, 8.05; N, 5.88). The 3*S*,4*S*; 3*R*,4*R* pair of diastereoisomers was separated from the 3*R*,4*S*; 3*S*,4*R* pair by chromatography over silica gel and then coupled with Boc-L-Val to give compound I by the methods developed for the synthesis of the corresponding statine analogues (Rich & Salituro, 1983). The 3*S*,4*S* diastereoisomer was separated from the 3*R*,4*R* diastereoisomer by chromatography: mp 189–191 °C; $R_f$ 0.45 (7% ethanol–ethyl acetate). $^1H$ NMR ($CDCl_3$) was consistent with the proposed structure (Anal. Calcd for $C_{33}H_{50}N_4O_6$: C, 61.96; H, 10.02; N, 10.32. Found: C, 62.28; H, 10.10; N, 10.21). Compound I inhibited porcine pepsin ($K_i = 10^{-6}$ M) in the previously described assay (Rich & Salituro, 1983).

*Stopped-Flow Kinetic Measurements.* Fluorescence-detected stopped-flow measurements were made as previously described (Auer & Glick, 1984). Fluorescence was excited at 295 nm and isolated by a Corning 7-59 filter, which passes light above 305 nm. The temperature was held to 22 ± 0.2 °C. Reactions were initiated by 1:1 mixing of solutions of protein in 0.05 M glycine–0.2 M NaCl (pH 6.02) or 0.05 M citrate–0.02 M NaCl (pH 8.25) with HCl solutions in 0.2 M NaCl, whose acid concentrations were adjusted to yield desired pH values. Actual pH values were determined after stopped-flow experiments on pooled samples of the product solutions. Either the inhibitor was premixed with pepsinogen, or it was included with the acid solution. Both zymogen and acid solutions contained 1% methanol. Data were handled and analyzed as before (Auer & Glick, 1984).

*Rates of Activation.* Rates of conversion to alkaline lability were determined as described by Al-Janabi et al. (1972) at 0, 10, and 20 °C. First-order rate constants were extracted by calculating the least-squares linear dependence of the logarithm of the proteolytic activity (minus its blank) upon time. These rate constants at each pH value were used to calculate energies of activation, again by a least-squares fitting method. We found that Arrhenius plots extended above 20 °C became nonlinear, and since rates at the higher temperatures are too fast for accurate manual sampling of activations near the pH optimum, we have confined our attention to the data between 0 and 20 °C, where plots are linear. Pepsin was assayed against denatured bovine hemoglobin (Chow & Kassell, 1968) and against Lys-Pro-Ala-Glu-Phe-($NO_2$)Phe-Arg-Leu (a gift of B. M. Dunn of the University of Florida, Gainesville, FL) in this same temperature range.

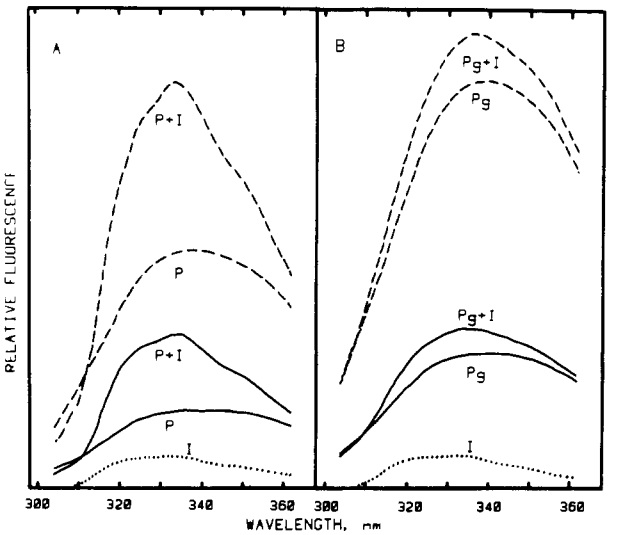


FIGURE 1: Emission spectra of 3.12 $\mu$M compound I (I) in the presence of pepsin (P) and pepsinogen (Pg). Corresponding emission spectra of the protein in the absence of compound I are also shown to allow correction for intrinsic fluorescence. (A) pH 2.30; pepsin concentrations are 0 (···), 1.36 (—), and 4.09 $\mu$M (– –). (B) pH 7.50; pepsinogen concentrations are 0 (···), 1.54 (—), and 4.62 $\mu$M (– –). Excitation was at 290 nm; solutions were in 0.2 M NaCl–0.44 M phosphate buffer–2% methanol at room temperature. The instrument was a SLM Aminco SPF 500 spectrofluorometer.

## Results

Compound I was synthesized in the course of studies to determine the effect of inhibitor side-chain structure on inhibitor potency (Rich & Sun, 1980; Rich & Salituro, 1983). It is an effective analogue of pepstatin (Umezawa et al., 1970) in which the isobutyl group of the critical statine residue (Rich & Salituro, 1983) has been changed by total synthesis to a naphthylmethylene group. Compound I is presumed to bind to the active site of pepsin because its $K_i$, $10^{-6}$ M, is consistent with that expected for Boc-terminal pepstatin analogues of this chain length (Rich et al., 1984) and because the corresponding Iva-L-Val-Hanp-L-Ala-Iaa derivative, formed by removing the Boc group and acylating with isovaleric anhydride, has a $K_i = 10^{-9}$ M against pepsin. Thus, replacement of the isobutyl side chain of statine by the naphthylmethylene group does not significantly alter the interaction with pepsin.

However, the presence of the naphthyl group in compound I provided an environmentally sensitive fluorescent group that could be used to monitor the entrance of the inhibitor into the enzyme active site during pepsin formation from pepsinogen. Compound I was examined in a static fluorescence experiment to test this possibility (Figure 1). The excitation spectrum of I overlaps that of the protein, as does its emission spectrum. Nevertheless, the enhancement of fluorescence in the presence of pepsin at pH 2.30 is sufficiently great to allow measurement of binding against the background of fluorescence of the protein (panel A). That is, the increase in fluorescence indicates the existence of a binding site with high affinity, involving intimate interaction of the fluorescent moiety with the protein. Furthermore, the binding is specific to the enzyme, since there is virtually no enhancement of fluorescence in the

Table I: Apparent First-Order Rate Constants for Genesis of the Binding Site

| expt | protein soln | acid soln | pH | rate const ± SD ($s^{-1}$) | no. of runs |
|---|---|---|---|---|---|
| 1 | 3 μM Pg | | 2.37 | 1.32 ± 0.09 | 6 |
| | 3 μM compd I | | | 0.30 ± 0.02 | |
| | 50 mM Gly | | | | |
| 2 | 3 μM Pg | | 2.41 | 1.18 ± 0.10 | 4 |
| | 3 μM compd I | | | 0.30 ± 0.02 | |
| | 50 mM citrate | | | | |
| 3 | 3 μM Pg | 3 μM compd I | 2.35 | 1.32 ± 0.14 | 4 |
| | 50 mM Gly | | | 0.37 ± 0.02 | |

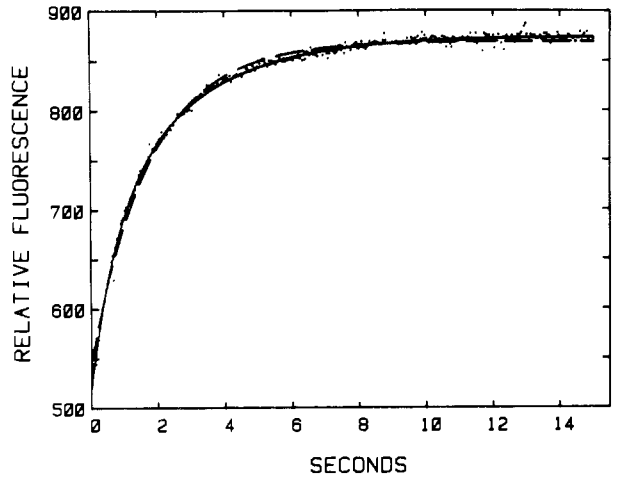


FIGURE 2: Example of a stopped-flow experiment. A 3 μM solution of pepsinogen in 0.05 M glycine–0.2 M NaCl–1% methanol was mixed with an equal volume of 3 μM compound I in dilute HCl in 0.2 M NaCl–1% methanol to produce a solution of pH 2.35. The raw data shown here were smoothed and analyzed as described under Materials and Methods. The data were fitted to a one-term exponential (– –) given by $Y_\infty = -869$, $A = -323.8 \pm 0.6$, and $k = 0.56 \pm 0.1$ $s^{-1}$, for which the mean square residual is 26.7. Alternatively, the data were fitted to a two-term exponential (—) described by $Y_\infty = -875$, $A_s = -155 \pm 8$, $k_s = 0.37 \pm 0.01$ $s^{-1}$, $A_f = -199 \pm 8$, and $k_f = 1.27 \pm 0.06$ $s^{-1}$, for which the mean square residual is 2.5. The symbol $Y_\infty$ is the fluorescence intensity at infinite time, the $A$'s are amplitudes, $k$'s are first-order rate constants, and the subscripts f and s refer to the fast and slow steps, respectively. On the fluorescence scale shown, the dark current was −1842.

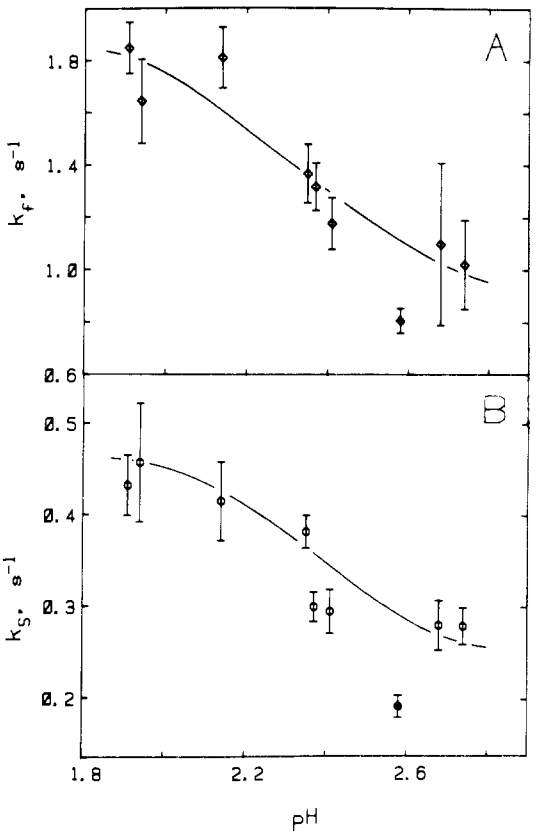


FIGURE 3: Apparent rate constants for formation of the binding site of pepsinogen vs. pH. Rate constants (±SD) for the fast event (panel A) and the slow event (panel B), obtained as in Figure 2, are shown as a function of pH. (Open symbols) Pepsinogen and I are each added at a concentration of 3 μM prior to mixing; (closed symbols) (pH 2.58) the corresponding concentrations are each 1 μM.

presence of the zymogen at pH 7.50 (panel B). This strongly suggests that pepsinogen does not bind I, although it cannot be ruled out that a zymogen–I complex forms without an attendant change in fluorescence.

The activation of pepsinogen in the presence of compound I was monitored in stopped-flow experiments. Runs were set up in two ways: with the zymogen and inhibitor premixed in the same syringe (referred to as experiments 1 and 2 in Table I) or with the zymogen and inhibitor kept in separate syringes until mixing (experiment 3). In both cases the zymogen was kept at neutral pH until mixing with acid. A typical run is shown in Figure 2. The transients were treated according to first-order kinetics. It was found that a single first-order decay furnished an inadequate fit to the data and that a two-term model was required (Figure 2). The satisfactory nature of the two-term fit is also evident from the values of the mean square residual for the two cases (see legend to Figure 2). Evidence for fluorescence changes occurring at shorter times than shown in Figure 2 was sought but was not observed. This suggests that early transient intermediates of pepsinogen cannot interact with compound I. Furthermore, there were no additional fluorescence changes at pH 1.94 up to 200 s.

The pH dependence of the observed fast and slow rate constants is shown in Figure 3. The constants increase by a factor of approximately 2 as the pH decreases in the range shown. In our previous work on the early events of pepsinogen activation, the data also fit a two-term exponential decay law (Auer & Glick, 1984). The pH dependence of the rate constants obtained in that work was far more striking than that depicted in Figure 3.

The experiment at pH 2.58 in Figure 3 was done with a mixture of pepsinogen and compound I at 1 μM each, before mixing, instead of the 3 μM level used in all the other work presented here. This has only a modest effect on the rate constants. If the reaction were, in fact, second order, rather than first order as we have assumed, the rates observed for the diluted reagents should have been only one-ninth as great. That the rate constants are not significantly diminished (Figure 3) assures us that the processes are, in fact, first order. Several experiments were also analyzed according to a second-order model, pepsinogen + I → complex, by nonlinear least-squares regression. It was found that, comparing the second-order model with the two-term exponential model, the mean square residual is much larger and the plot of residuals vs. time exhibits a characteristic pattern for the former, whereas it is random for the latter (not shown). Furthermore, the second-order rate constant obtained for the dilute reagents is 1.7 times larger than that found at the higher concentrations. These findings militate against interpreting the results according to a second-order reaction.

Control experiments performed under similar conditions, but with pepstatin or with no inhibitor being present, showed no transients. This allows us to conclude that the fluorescence changes observed are indeed due to binding of the inhibitor to the acidified zymogen. Further evidence in support of this

Scheme I: Models for Origin of a Two-Term Exponential Decay[a]

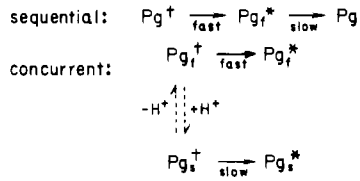


[a] In either model, the starting species is a transient intermediate appearing after the protonation of pepsinogen upon acidification to a low pH. Combination of Pg species with I is left to implication in these models (see text). Species marked by daggers (†) have no I bound or have I bound with no increase in fluorescence intensity. Species marked by asterisks (*) have I bound in the binding site. The use of the broken arrows for the protonation step in the concurrent model is considered in the text.

conclusion was obtained by using the 3*R*,4*R* form of compound I, which is assumed to bind more weakly than the 3*S*,4*S* form. The fluorescent amplitude change was considerably weaker than that obtained with the 3*S*,4*S* enantiomer, in accord with its supposed weaker binding to pepsin. The possibility that protein aggregation occurs was ruled out, as it was before (Auer & Glick, 1984), by observing constant light scattering intensity over the time course of the runs.

## Discussion

The fluorescence-detected processes characterized here are ascribed to the genesis of a binding site for compound I. Since these processes occur during activation, since the fluorogenic probe is known to bind tightly to the pepsin active site, and since the bond cleavage during activation is generally acknowledged to be closely related to substrate cleavage during pepsin catalysis, we have assumed that these processes are integral to the activation of pepsinogen. In support of this view, we recall that no additional fluorescence change was observed up to 200 s. Since this time span corresponds to the time required for complete activation (see Scheme III and Table II, below), the fluorescence change observed by us must represent the full fluorescence enhancement developed by compound I when it binds to pepsin (see Figure 1). Therefore, the rate of binding of compound I monitors the genesis of the binding site during activation. The binding site must be similar to the active site of pepsin in view of (a) the inhibitory properties of compound I, (b) the weaker effect observed with the 3*R*,4*R* form, and (c) the competitive effect of pepstatin leading to loss of an observable transient. The intrinsic fluorescence of pepsinogen is transparent to this process, for we failed to observe any effects in the absence of compound I both in our earlier work (Auer & Glick, 1984) and in this investigation.

In order to understand the origin of the two processes detected in our experiments, we shall consider a sequential model and a concurrent model, as was done in our previous work on the early events in pepsinogen activation (Scheme I). In either case, the starting species $Pg^{\dagger}$, $Pg_f^{\dagger}$, and $Pg_s^{\dagger}$ are either the direct products that arise as a result of the early events in pepsinogen activation (Auer & Glick, 1984) or further products arising from those species by as yet uncharacterized processes. It is assumed that the various $Pg^{\dagger}$ species have sufficiently weak affinity for compound I that complex formation may be ignored or else that they bind compound I in a configuration that does not enhance the fluorescence of the naphthyl fluorophore. $Pg_f^{*}$ and $Pg_s^{*}$, on the other hand, are assumed to bind compound I avidly, leading to complex formation and enhancement of the fluorescence. For the sake of this discussion, the bimolecular step(s) leading to complex formation is (are) left as implicit in the models of Scheme I; we shall return to consider this point further below.

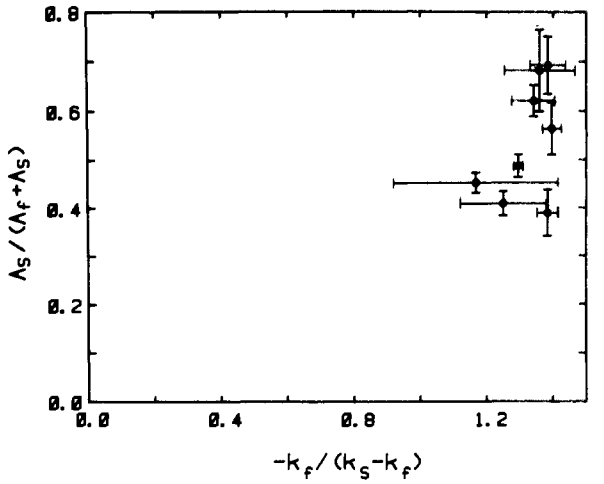


FIGURE 4: Test of kinetic data for fit to the sequential model. The symbols have the meanings described in the text for eq 1. Standard deviations for the factors defining the abscissa and ordinate are shown.

In order to select between models, we consider first the sequential case. A sequential first-order model predicts that the amplitudes are related to the rate constants in specific ways; in particular, the amplitude of the slow step $A_s$ is given by Espenson (1981):

$$A_s = (F_s^* - F_f^*)[Pg]_0 k_f/(k_s - k_f) \quad (1)$$

Here, $F_f^*$ and $F_s^*$ are the quantum yields of compound I when complexed with $Pg_f^*$ and $Pg_s^*$, respectively; $[Pg]_0$ is the total concentration of Pg present, and $k_f$ and $k_s$ are the apparent rate constants for the fast and slow steps, respectively. If the sequential model is to account adequately for our results, a plot of $A_s$ vs. $k_s/(k_s - k_f)$, according to eq 1, should be linear and pass through the origin, assuming that $F_s^*$ and $F_f^*$ are independent of pH in the range considered here. Such a plot is presented in Figure 4 for data obtained in the runs shown in Figure 3. In order to account for variable instrument settings in different runs, $A_s$ has been normalized by the factor $(A_s + A_f)^{-1}$. It is evident from Figure 4 that the data are not in accord with eq 1, for the points bear no clear correlation with each other. It may be concluded, therefore, that the sequential model is not appropriate for this system.

The concurrent model depicted in Scheme I indicates that the starting species $Pg_f^{\dagger}$ and $Pg_s^{\dagger}$ are related to each other by a protonation step. It is supposed that the two conjugate acid–conjugate base species of $Pg^{\dagger}$ are additionally in distinct conformations, in order to account for the difference in their rates; the basis for this assumption is discussed below. The relative populations of $Pg_f^{\dagger}$ and $Pg_s^{\dagger}$ at any pH value should be given by the Henderson–Hasselbalch equation. Therefore, the amplitudes of the fast and slow steps, which are proportional to $[Pg_f]$ and $[Pg_s]$, respectively, should give a straight line in a Henderson–Hasselbalch plot. Our data are presented in this way in Figure 5. A straight line is indeed obtained with a slope of 0.89 ± 0.15 and an apparent $pK_a$ of 2.24 ± 0.03. (It should be noted, however, that when we extended these experiments above pH 3, points at pH 3.01 and 3.16 were found to fall below the line shown in Figure 5.) Thus, a single protonation is involved in the transformation between $Pg_f^{\dagger}$ and $Pg_s^{\dagger}$, and if the quantum yields of I in $Pg_f^*$ and $Pg_s^*$ are not significantly different, the $pK_a$ of the acidic group in question is approximately 2.2. It should be recalled that in considering these two models for the early steps in the activation of TNS-pepsinogen the concurrent model based on a protonic

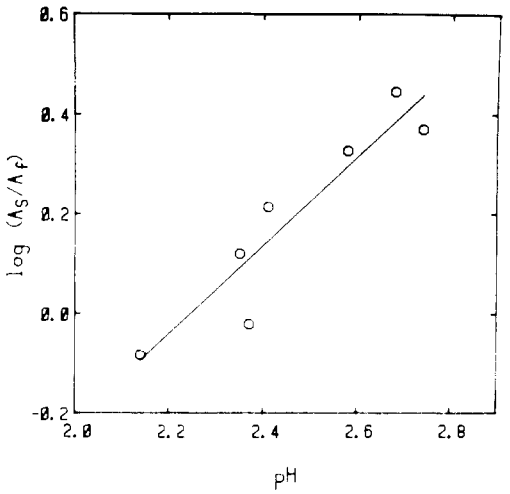


FIGURE 5: Test of kinetic data for fit to the concurrent model. The logarithms of the ratio of the amplitudes for the slow and fast events measured as in Figure 2 are shown vs. pH.

Scheme II: Alternative Kinetic Models for Interaction of Compound I with Transient Intermediates of Pepsinogen[a]

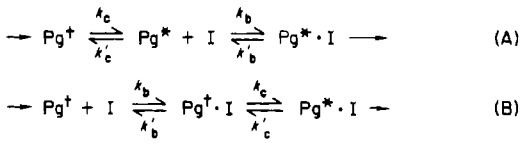


[a] It is assumed that the formation of Pg†·I results in no enhancement of fluorescence of I.

equilibrium was also found to be consistent with the data (Auer & Glick, 1984), with a slope indicating a single protonation event and a p$K_a$ of 2.0. It may be that the same group on pepsinogen is responsible for the protonic equilibria that we detect in these two kinetic time ranges.

One should recognize that a rapid protonic equilibrium between otherwise identical protein molecules cannot explain our results. If this were the case, as $Pg_f^\dagger$ was preferentially depleted by its rapid reaction to $Pg_f^*$, the protonic equilibrium would be displaced in its favor, drawing off $Pg_s^\dagger$ prior to the latter's transformation to $Pg_s^*$. This would not permit us to fit the Henderson–Hasselbalch equation. Rather, we conclude that the protonic equilibrium is established at some point prior to the formation of Pg† (Scheme I) and then evidently is locked in by specific conformational changes. This notion underlies the use of the broken arrows to express the protonation in Scheme I. After this time, proton-mediated conformational reequilibration is kinetically insignificant, so that the fate of the protein molecule is determined. If this equilibrium is established prior to the rapid steps determined in our earlier work (Auer & Glick, 1984), the identity of the p$K_a$ values and of the molecularity for protonation determined there and in this study is easily understood, since they indeed refer to the same early equilibration process.

A more detailed consideration of the process observed in the present experiments suggests two possible models for transformation of Pg† to Pg* and the binding of compound I (see Scheme II). In this scheme, Pg† and Pg* are one or the other of $Pg_f^\dagger$ and $Pg_s^\dagger$ and $Pg_f^*$ and $Pg_s^*$, respectively. $k_c$ and $k_c'$ are the forward and reverse first-order rate constants for the acid-induced conformational change, and $k_b$ and $k_b'$ are the rate constants for association and dissociation, respectively, of the complex of Pg with I. $k_c'$ is most likely small, and it is assumed that the reverse reaction does not occur to any significant extent during the activation of pepsinogen. $k_b/k_b'$ represents a relatively rapid equilibration of I between

Scheme III: Proposed Pathways for Pepsinogen Activation[a]

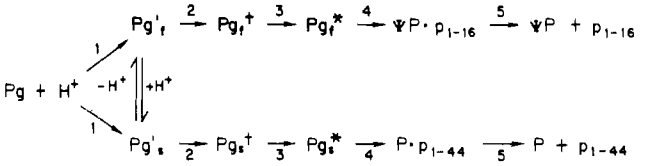


[a] Representative values for the rate constants characterizing steps 1–5 are shown in Table II.

Table II: Events of Pepsinogen Activation

| step[a] | process | $k$ ($s^{-1}$) | conditions | ref |
|---|---|---|---|---|
| 1 | diffusion-limited protonation | $4 \times 10^7$ | pH 2.4, 22 °C | Jencks, 1969 |
| 2 | early fluorescence changes | 70.0<br>200.0 | pH 2.4, 22 °C | Auer & Glick, 1984 |
| 3 | formation of the binding site | 0.3<br>1.3 | pH 2.4, 22 °C | this paper |
| 4 | conversion to alkaline lability | 0.025 | pH 2.4, 28 °C | Al-Janabi et al., 1972 |
| 5[b] | dissociation of activation peptide | 0.005 | pH 2.4, 22 °C | Twining et al., 1981 |

[a] Steps refer to events depicted in Scheme III. [b] Measured on spin-labeled pepsinogen, for which the rate constant for conversion to alkaline lability is 0.05 $s^{-1}$ at pH 2.4, 22 °C.

free and bound forms. In model A, I binds to Pg* after creation of the binding site, whereas in model B I complexes with Pg† before the appearance of this site.

Models A and B lead to rate equations that are easily solved under conditions of relaxation of perturbation. The rate constants may then be determined by varying the concentration of one of the two reactants. Unfortunately, such procedures are difficult to apply in our case for the following reasons. First, in each model, we must resolve not one but two reactions, those of $Pg_f^\dagger$ and $Pg_s^\dagger$. Second, both Pg and I undergo excitation and emission of fluorescence at the same wavelengths. This would interfere with rigorous analysis of the rates by varying reactant concentrations, due to interference from the second reactant. And third, our experiments are done under conditions far from those valid for relaxation perturbation. For these reasons, it was deemed unproductive to attempt to unravel the kinetics of our system further. We recognize that as a result the rate constants depicted in Figure 3 may not accurately represent the true values of $k_c$ for the Pg† to Pg* transformation. It must be noted, however, that in the experiment at pH 2.58, in which both Pg and I are present at one-third the concentrations used in the other experiments, there is only a slight effect on the apparent rate constants (Figure 3). Therefore, we must conclude that the $k_b/k_b'$ equilibrium does not drastically affect the apparent rate constants. Furthermore, the rates observed in this work are 2 orders of magnitude slower than the preceding step and 1 order of magnitude faster than the following step (see below). Therefore, it is unlikely that any more rigorous analysis of the present reaction would lead to a value of $k_c$ that would require the interchanging of this step with either of its neighbors shown in Scheme III. We thus affirm that these experiments have indeed detected a hitherto uncharacterized step in the pathway for the activation of pepsinogen, which we interpret as the coalescence or creation of the binding site.

One may now include this newly observed step in an expanded description of the activation of pepsinogen. This is shown in Scheme III and Table II, where rate constants are given for pH 2.4, 22 °C, except as noted below. All the rates in Table II are sufficiently different from one another for us

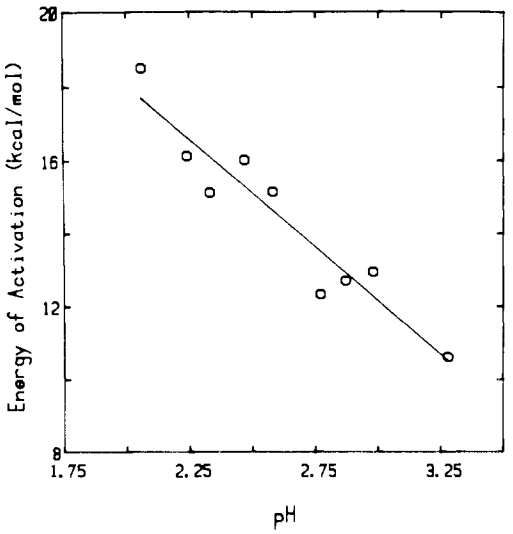


FIGURE 6: Energy of activation vs. pH for pepsinogen activation. The rate of conversion of potential activity to lability at pH 8.5 was taken to be the rate of activation. From the increase of these rates from 0 to 20 °C at several pH values, the activation energies were calculated.

to conclude that they represent distinct steps in pepsinogen activation. In this scheme, Pg represents pepsinogen prior to acidification, and Pg′, $Pg^{\dagger}$, and Pg* are the several transient intermediate species of Pg after acidification. The rate of protonation, step 1, is too fast to observe. The protonic equilibrium and its concomitant conformational equilibrium relating $Pg_f'$ and $Pg_s'$, which we proposed above, is included. We have identified two rapid changes in intrinsic fluorescence following protonation, step 2 (Auer & Glick, 1984). The rate of formation of the binding site, step 3, is reported here. The conventionally observed activation rate, that for conversion to alkaline lability, step 4, was determined by Al-Janabi et al. (1972) at 28 °C. The actual rate of peptide bond cleavage during activation has never been directly observed, but it may be that this event is identical with the conversion to alkaline lability. The transient intermediates of Pg lead ultimately to pseudopepsin, ΨP, the first enzymatically active product (Dykes & Kay, 1976; Christensen et al., 1977) as shown hypothetically on the upper line for the fast-reacting pathway. The activation peptide $p_{1-16}$ is comprised of the first 16 amino-terminal residues of Pg. In this pathway, pepsin eventually arises by bimolecular processing to remove a total of 44 amino-terminal residues from the original zymogen (not shown). Kageyama and Takahashi (1983) have proposed that pepsinogen may also undergo a single acid-initiated cleavage directly to pepsin, P, by cleavage of the entire amino-terminal peptide 1–44, $p_{1-44}$. This proposal is incorporated into Scheme III as steps 4 and 5 of the lower, slow-reacting pathway. Thus, we are proposing that the concurrent fast and slow pathways that we have demonstrated to exist at steps 2 and 3 continue through steps 4 and 5. At this time, it must be emphasized that assignment of the fast-reacting, high-pH pathway to the cleavage of $p_{1-16}$ and of the slow-reacting, low-pH pathway to the cleavage of $p_{1-44}$ is entirely arbitrary and is subject to change.

We wished to assemble data to support the hypothesis that pepsinogen activates by two parallel pathways. A distinguishing characteristic of a reaction pathway might be its Arrhenius energy of activation, $E_a$. If the proportions of pepsinogen activated by each of the two pathways vary with pH, the $E_a$, determined from the temperature dependence of conversion to alkaline lability, should also vary with pH. When the measurements were made at pH values below 3, a strong dependence upon pH was seen (Figure 6).[2] (Above pH 3 the data were irreproducible, and no reliable results can be reported.) While this finding is consistent with the postulate that two species related by a protonic dissociation undergo the process shown in step 4, it is not decisive, as there are alternative explanations. However, the findings are unlikely to be due to a change with temperature of the $pK_a$ of a critical dissociating group, because the $\Delta H°$ for protonation of a carboxylate is close to zero (Edsall & Wyman, 1958a,b).[3]

In our current view, two conformations of pepsinogen of roughly equal stability may undergo activation. These conformations are separated by a significant energy barrier, but the relative stabilities of these two conformations may be altered by protonation of a single group with $pK_a$ near 2. The effect of protonation is to shift the balance toward that conformation which forms the binding site more slowly and thus imposes on this process the pH dependence we find (Figure 3). In examining an earlier event of pepsinogen activation, we found a similar basis for the pH dependence of its rate, and we venture to propose that when the site of peptide bond cleavage is examined, a similar basis for its pH dependence will be found.

## ACKNOWLEDGMENTS

We are grateful to Prof. B. M. Dunn for his generous gift of an octapeptide pepsin substrate. We gratefully acknowledge support from the Medical College of Wisconsin Advisory Computer Committee.

**Registry No.** I (3*S*,4*S* diastereomer), 100994-43-2; I (3*R*,4*R* diastereomer), 101053-49-0; Boc-Hanp-OEt (3*S*,4*S*;3*R*,4*R* diastereomeric pair), 100994-44-3; Boc-Hanp-OEt (3*R*,4*S*;3*S*,4*R* diastereomeric pair), 100994-48-7; Boc-Hanp-OH (cyclohexylammonium salt), 100944-47-6; Boc-L-Val, 13734-41-3; Boc-β-naphthylalanine ethyl ester, 100994-45-4; pepsinogen, 9001-10-9.

## REFERENCES

Al-Janabi, J., Hartsuck, J. A., & Tang, J. (1972) *J. Biol. Chem. 247*, 4628–4632.

Arnon, R., & Perlmann, G. E. (1963) *J. Biol. Chem. 238*, 653–656.

Auer, H. E., & Glick, D. M. (1984) *Biochemistry 23*, 2735–2739.

Chow, R. B., & Kassell, B. (1968) *J. Biol. Chem. 243*, 1718–1724.

Christensen, K. A., Pedersen, V. B., & Foltmann, B. (1977) *FEBS Lett. 76*, 214–218.

Dykes, C. W., & Kay, J. (1976) *Biochem. J. 153*, 141–144.

Edsall, J. T., & Wyman, J. (1958a) *Biophysical Chemistry*, Vol. 1, pp 452–453, Academic, Ney York.

Edsall, J. T., & Wyman, J. (1958b) *Biophysical Chemistry*, Vol. 1, pp 524–527, Academic, New York.

Espenson, J. H. (1981) *Chemical Kinetics and Reaction*

[2] The variation with pH of the site of initial bond cleavage in pepsinogen activation, which we suggest may occur, has its parallel in pepsin catalysis: the pH optimum for hydrolysis by pepsin varies with the substrate (Fruton, 1976). To see if the parallel between pepsinogen activation and pepsin-hydrolyzed catalysis extends further, we measured the $E_a$ for pepsin-catalyzed hydrolysis. With denatured hemoglobin as a substrate, $E_a$ varied from 9.8 kcal/mol at pH 2.01 to 15.4 kcal/mol at pH 3.07; with the octapeptide Lys-Pro-Ala-Glu-Phe-($NO_2$)Phe-Arg-Leu, it varied from 10.1 kcal/mol at pH 2.04 to 24.6 kcal/mol at pH 3.07.

[3] Any contribution to $E_a$ from a carboxylate would have to have (a) a large value and (b) a strong pH dependence in this pH range. Neither of these requirements is likely to be fulfilled because the values of $\Delta H°$ for carboxyl ionizations in hemoglobin and in α-amino acids have been shown to be small, in the range of 0–2 kcal/mol (Edsall & Wyman, 1958a,b).

*Mechanisms*, pp 65–67, McGraw-Hill, New York.
Fruton, J. S. (1976) *Adv. Enzymol. Relat. Areas Mol. Biol. 44*, 1–36.
Glick, D. M., Valler, M. J., Rowlands, C. C., Evans, J. C., & Kay, J. (1982) *Biochemistry 21*, 3746–3750.
Jencks, W. P. (1969) *Catalysis in Chemistry and Enzymology*, pp 207–211, McGraw-Hill, New York.
Kageyama, T., & Takahashi, K. (1983) *J. Biochem. (Tokyo) 93*, 743–754.
Marciniszyn, J., Jr., Huang, J. S., Hartsuck, J. A., & Tang, J. (1976) *J. Biol. Chem. 251*, 7095–7102.
Rich, D. H., & Sun, E. T. O. (1980) *Biochem. Pharmacol. 29*, 2205–2212.
Rich, D. H., & Salituro, F. G. (1983) *J. Med. Chem. 26*, 904–910.
Rich, D. H., Sun, E. T., & Boparai, A. S. (1978) *J. Org. Chem. 43*, 3624–3626.
Rich, D. H., Salituro, F. G., Holladay, M. W., & Schmidt, P. G. (1984) in *Conformationally Directed Drug Design* (Vida, J. A., & Gordon, M., Eds.) pp 211–237, American Chemical Society, Washington, DC.
Twining, S. S., Sealy, R. C., & Glick, D. M. (1981) *Biochemistry 20*, 2375–2379.
Umezawa, H., Aoyagi, T., Morishama, H., Matsuzaki, M., Hamada, M., & Takeuchi, T. (1970) *Antibiotics 23*, 259–269.

# Activation and $CO_2$ Exchange Kinetics of Ribulose-1,5-bisphosphate Carboxylase/Oxygenase: Negative Cooperativity with Respect to $Mg^{2+}$

William R. Belknap[‡] and Archie R. Portis, Jr.*
*Department of Agronomy, University of Illinois, and U.S. Department of Agriculture, Agricultural Research Service, Urbana, Illinois 61801*

*Received June 10, 1985; Revised Manuscript Received October 28, 1985*

ABSTRACT: We have reexamined the activation kinetics of spinach ribulose-1,5-bisphosphate carboxylase/oxygenase (rubisco) with respect to $CO_2$ and $Mg^{2+}$. Negative cooperativity (Hill coefficient = 0.65) with respect to the $Mg^{2+}$ dependence of rubisco activation was observed both in equilibrium studies and in kinetic determinations of the pseudo-first-order rate constants. No cooperativity effects (Hill coefficient = 1) were observed with respect to the $CO_2$ dependence of activation. The effects of $Mg^{2+}$ and $CO_2$ on the exchange kinetics of the activator $CO_2$ of rubisco were also analyzed by utilization of the transition-state analogue 2-carboxyarabinitol 1,5-bisphosphate to trap the $CO_2$ moiety on the enzyme. Rate constants for exchange at steady-state activation determined in the presence of different $Mg^{2+}$ and $CO_2$ concentrations were also consistent with negative cooperativity with respect to $Mg^{2+}$ binding and indicate an equilibrium between active and inactive forms of the enzyme during steady-state activation. The presence of negative cooperativity in activation with respect to $Mg^{2+}$ but not with respect to $CO_2$ may indicate that the observed cooperativity effects are due to allosteric interactions in activation rather than a heterogeneity of the activator sites on the purified enzyme.

Ribulose-1,5-bisphosphate carboxylase/oxygenase (rubisco) (EC 4.1.1.39) is a bifunctional enzyme that catalyzes either the carboxylation or the oxygenation of the substrate ribulose 1,5-bisphosphate (RuBP). The enzyme from higher plants is large (550 kDa) and is composed of eight large and eight small subunits (Miziorko & Lorimer, 1983). Both the carboxylation and oxygenation activities are associated with the large subunit. The function of the small subunit, while proposed to be regulatory, is unknown.

The activation state of the enzyme has also been shown to be modulated in vivo, and the extent of rubisco activation may limit overall photosynthesis (Perchorowicz et al., 1981). Kinetic evidence (Lorimer et al., 1976; Laing & Christeller, 1976) has established that an inactive form of the enzyme can be activated in vitro by the ordered addition of first $CO_2$ and then $Mg^{2+}$. The activating $CO_2$ has been shown to bind to an activator site on the enzyme, which results in carbamate formation on a lysyl residue (Lorimer & Miziorko, 1980). The $CO_2$ bound during the activation process has been shown to be distinct from that involved in catalysis (Lorimer, 1979; Miziorko, 1979).

In their pioneering studies on the kinetics of rubisco activation, Lorimer et al. (1976) obtained evidence that the binding of $CO_2$ to the enzyme is the rate-limiting step in the activation process, followed by a rapid equilibration of the enzyme–$CO_2$ complex with $Mg^{2+}$ to form the catalytically competent enzyme–$CO_2$–$Mg^{2+}$ complex. The following model was proposed to account for the data obtained:

$$E_i + CO_2 \underset{k_2}{\overset{k_1}{\rightleftharpoons}} E\text{–}CO_2 + Mg^{2+} \underset{k_4}{\overset{k_3}{\rightleftharpoons}} E_a \qquad (1)$$

where $E_i$ represents an inactive form of the enzyme and $E_a$ represents the catalytically competent ternary complex (enzyme–$CO_2$–$Mg^{2+}$). Laing and Christeller (1976) derived values for the individual rate constants of the soybean enzyme by combining the pseudo-first-order rate constants for activation and equilibrium measurements at various $CO_2$ and $Mg^{2+}$ concentrations with measurements of the decay rate of the activated enzyme in the absence of $Mg^{2+}$. $Mg^{2+}$-dependent variation in the derived rate constants was reported. This variation was attributed to possible changes in rubisco acti-

* Address correspondence to this author at USDA, ARS, Department of Agronomy, University of Illinois.
‡ Present address: Department of Molecular Genetics and Cell Biology, University of Chicago, Chicago, IL 60637.

0006-2960/86/0425-1864$01.50/0 